

Superconducting Analogues of Quantum Optical Phenomena: Schrödinger Cat States and Squeezing in a SQUID Ring.

M. J. Everitt,^{*} T. D. Clark,[†] P. B. Stiffell, R. J. Prance, and H. Prance

*Centre for Physical Electronics and Quantum Technology,
School of Science and Technology, University of Sussex, Brighton, Sussex, BN1 9QT, U.K.*

A. Vourdas

Department of Computing, Bradford University, Bradford, West Yorkshire, BD7 1DP, UK.

J. F. Ralph

*Department of Electrical and Electronic Engineering,
Liverpool University, Brownlow Hill, Liverpool, L69 3GJ, U.K.*

(Dated: May 6, 2019)

In this paper we explore the quantum behaviour of a SQUID ring which has a very strong Josephson coupling energy. We show that the eigenfunctions of the Hamiltonian for the ring can be used to create Schrödinger cat states. We also show that the ring potential may be utilised to squeeze coherent states. With the SQUID ring as a strong contender as a device for manipulating quantum information, such properties may be of great utility in the future. However, as with all candidate systems for quantum technologies, decoherence is a fundamental problem. In this paper we apply an open systems approach to model the effect of coupling a quantum mechanical SQUID ring to a thermal bath. We use this model to demonstrate the manner in which decoherence affects the quantum states of the ring.

PACS numbers: 74.50+r 85.25.Dq 03.65.-w 42.50.Dv

Introduction

In two recent publications [1, 2] we reported on the theoretical description of a quantum mechanical SQUID ring (here, a thick superconducting ring enclosing a single Josephson weak link device) coupled to quantised electromagnetic field (em) oscillator modes. In this work we emphasised that the SQUID ring could be used to control various quantum phenomena involving each of the circuit components of the coupled system via the static magnetic bias flux (Φ_x) applied to the ring. These included frequency conversion between the em modes and quantum entanglement extending across the system, both with relevance to emerging quantum technologies based on Josephson devices [3, 4, 5, 6, 7, 8, 9, 10, 11, 12, 13]. Furthermore, work by Friedman et al on SQUID rings has highlighted another phenomenon of potentially great significance to these incipient technologies, namely Schrödinger cat states [14]. As will become apparent, the creation and control of such states is a natural application for a SQUID ring.

In this paper we consider the creation and control of Schrödinger cat states in a SQUID ring alone, uncoupled to any em oscillator modes. First, we consider the spectral properties of the ring Hamiltonian. Then we observe that at certain points in the bias flux (Φ_x) applied to the ring the eigenfunctions of this Hamiltonian form

Schrödinger cat states. We show that a strong enough level of dissipation may destroy the quantum nature of these cat states, whilst leaving the flux in the SQUID ring in a statistical mixture of two macroscopically distinguishable states. Following this we demonstrate that superposition states of a SQUID ring can be used to create (form) a controllable Schrödinger cat state. In addition to this demonstration of Schrödinger cat states, we show that a SQUID ring with a sufficiently large Josephson coupling term in its potential can be used to squeeze coherent states. In this it is apparent that physical phenomena associated with SQUID rings, and with quantum circuits built around SQUID rings, have analogies with effects well known in the field of quantum optics. Indeed the SQUID ring can be viewed as a non-linear medium which, for example, can be utilised to generate entanglements, frequency conversion, cat states and squeezing. However, the SQUID ring has significant advantages over the generally weakly polynomial non-linear media of quantum optics which are usually weakly coupled to external electromagnetic (em) fields. Thus, it is extremely non-perturbative in nature (and concomitantly capable of inducing extremely non-linear behaviour [1, 2, 15]) with a coupling to em modes that can be adjusted by means of an external bias flux. This would appear to make the SQUID a prime candidate for future developments in what is, in effect, highly non-perturbative quantum optics, albeit at much lower frequencies. In practice these frequencies would typically be much less than a THz for low critical temperature superconductors.

^{*}Electronic address: m.j.everitt@sussex.ac.uk

[†]Electronic address: t.d.clark@sussex.ac.uk

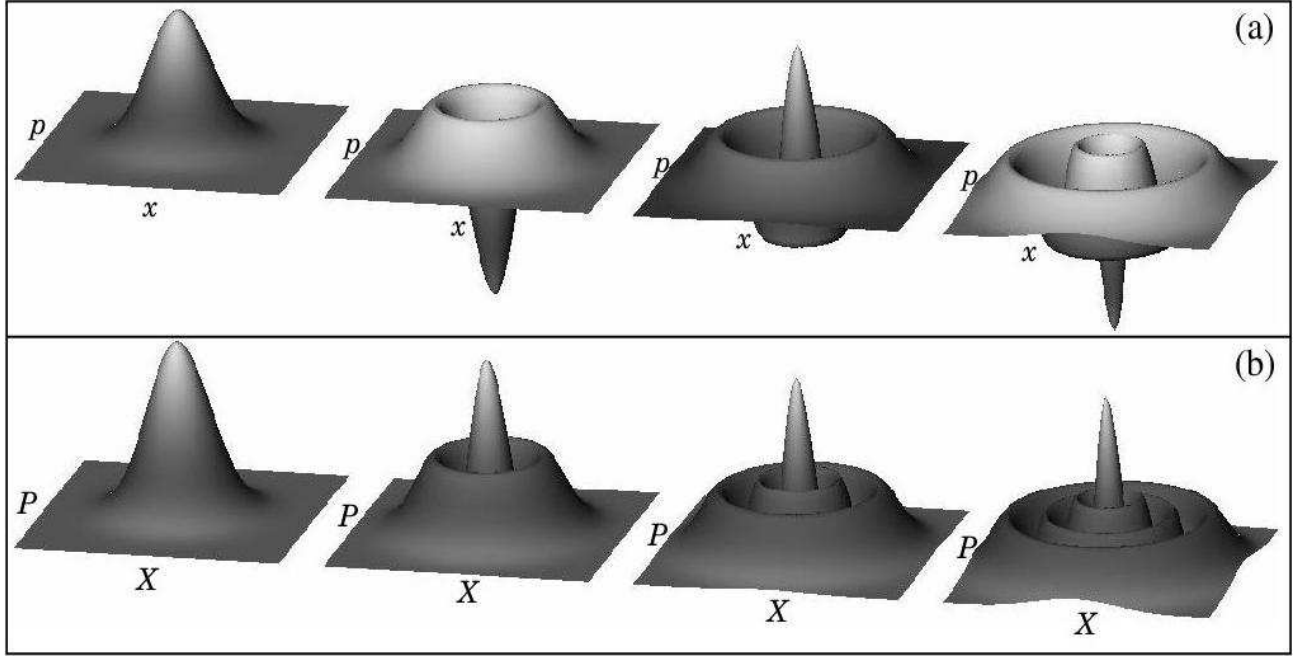


FIG. 1: (a) Wigner and (b) absolute value of the Weyl functions of the first four energy eigenstates of the simple harmonic oscillator (increasing in energy from left to right).

Background

Wigner and Weyl Functions

Although the Wigner and Weyl functions are familiar to those working in the field of quantum optics [16, 17, 18], their use in the quantum description of Josephson weak link circuits, and in particular SQUID rings, appears to be rather limited. The Wigner function is defined to be

$$\begin{aligned} W(x, p) &= \frac{1}{2\pi} \int d\zeta \left\langle x + \frac{1}{2}\zeta \left| \rho \right| x - \frac{1}{2}\zeta \right\rangle \exp(-i\zeta p) \\ &= \frac{1}{2\pi} \int d\zeta \left\langle p + \frac{1}{2}\zeta \left| \rho \right| p - \frac{1}{2}\zeta \right\rangle \exp(-i\zeta x) \end{aligned}$$

where ρ is the density operator describing the state of the system with conjugate variables position (x) and momentum (p). Physically, the Wigner function can, to some extent, be considered as a generalisation of the wavefunction of the quantum system under study in which we are provided with information in both position and momentum space. We note that the Wigner function may, and often does, take on negative as well as positive values. An important and characteristic feature of the Wigner function is that the quantum correlations between the macroscopically distinct components of a Schrödinger cat state can be seen in an obvious and graphical way, i.e. these correlations will appear in the Wigner function as interference terms between the states of the cat in the $x - p$ phase plane.

By contrast, the Weyl function is defined as

$$\begin{aligned} \tilde{W}(X, P) &= \frac{1}{2\pi} \int d\zeta \left\langle \zeta + \frac{1}{2}X \left| \rho \right| \zeta - \frac{1}{2}X \right\rangle \exp(-i\zeta P) \\ &= \frac{1}{2\pi} \int d\zeta \left\langle \zeta + \frac{1}{2}P \left| \rho \right| \zeta - \frac{1}{2}P \right\rangle \exp(-i\zeta X) \end{aligned}$$

It is apparent here that the Weyl function of a state is equal to the overlap of the displaced state with the original state so that X and P are considered as increments in position and momentum. As can be seen, the Weyl function is a generalised autocorrelation function; it is also the two dimensional Fourier transform of the Wigner function. Thus, just as the Wigner function highlights the regions in the $x - p$ plane where the wavefunction amplitude is significant, the Weyl function tells us where there exists a significant amplitude for correlations between intervals of $\Delta x (= X)$ and $\Delta p (= P)$ in this plane. A more detailed discussion and review of Wigner and Weyl functions, and the relationship between them, can be found in the literature [18, 19].

For those unfamiliar with these functions we provide a specific example in figure 1. Here, we have plotted the Wigner functions for the first four energy eigenstates of the simple harmonic oscillator together with the absolute values of their associated Weyl functions. We note that the Weyl function is, in general, complex valued. In this paper, therefore, we only ever plot its absolute value since, for our purposes, this provides us with sufficient information about the correlations of the wavefunction.

The SQUID Ring Hamiltonian

Over the last two decades SQUID rings, viewed as single, macroscopic, quantum objects, have been the subject of considerable attention theoretically. In early studies the focus was primarily on time independent properties and the interaction of SQUID rings with external environments [15, 20, 21]. Of late there has been much interest in time dependent behaviour, for example, in solving the time dependent Schrödinger equation (TDSE) for a SQUID ring in the presence of a microwave field [22, 23]. Recently, significant efforts have been devoted to the experimental measurement and control of Schrödinger cat states in SQUID rings [14]. In this paper we proceed to develop a theoretical description of cat states in SQUID rings, borrowing on techniques that are commonly used in quantum optics. We extend the usefulness of this description by considering quantum mechanical squeezed states in SQUID rings. For both cat states and squeezing in these rings we also discuss the effect of dissipation (decoherence).

In the widely used lumped component model of a SQUID ring [15, 20] the Hamiltonian takes the form.

$$H = \frac{Q^2}{2C} + \frac{(\Phi - \Phi_x)^2}{2\Lambda} - \hbar\nu \cos\left(\frac{2\pi\Phi}{\Phi_0}\right) \quad (1)$$

where Φ and Q are, respectively, the magnetic flux threading the ring and the electric displacement flux across the weak link (with $[\Phi, Q] = i\hbar$), $\hbar\nu/2$ is the matrix element for Josephson tunnelling through the weak link (with critical current $I_c = 2e\nu$), $\Phi_0 = h/2e$ is the superconducting flux quantum and Λ and C are, respectively, the ring inductance and the capacitance of the weak link in the ring.

Introducing a unitary translation operator $\mathbb{T} = \exp(-i\Phi_x Q/\hbar)$, we can then write down the ring Hamiltonian as

$$H' = \mathbb{T}^\dagger H \mathbb{T} = \frac{Q^2}{2C} + \frac{\Phi^2}{2\Lambda} - \hbar\nu \cos\left(2\pi\frac{\Phi + \Phi_x}{\Phi_0}\right) \quad (2)$$

where it is clear that as $\hbar\nu \rightarrow 0$ the system behaviour reduces to that of a simple harmonic oscillator. Given the relation between our system and the simple harmonic oscillator we now define creation and annihilation operators in the usual way, i.e. as

$$a = \sqrt{\frac{C\omega}{2\hbar}} \left(\Phi - \frac{i}{C\omega} Q \right), a^\dagger = \sqrt{\frac{C\omega}{2\hbar}} \left(\Phi + \frac{i}{C\omega} Q \right).$$

These raising and lowering operators, as used in quantum optics, then allow us to write the ring Hamiltonian in a more convenient form. We also choose to express it in dimensionless units, normalised to $\hbar\omega$, where $\omega/2\pi = 1/2\pi\sqrt{\Lambda C}$ is the SQUID ring oscillator frequency. This takes the form

$$\mathcal{H} = \left(a^\dagger a + \frac{1}{2} \right) - \frac{\nu}{\omega} \cos\left(\frac{2\pi}{\Phi_0} \sqrt{\frac{\hbar}{2C\omega}} [a + a^\dagger] + 2\pi\varphi_x \right) \quad (3)$$

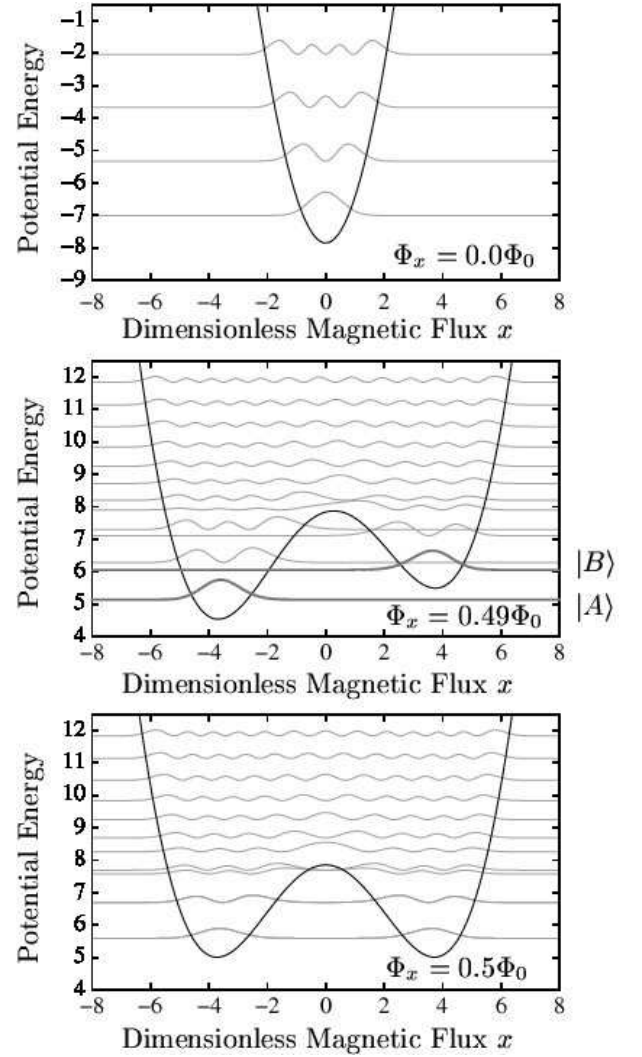


FIG. 2: Potential energy of a SQUID ring with parameter values $C = 5 \times 10^{-15}$ F, $\Lambda = 3 \times 10^{-10}$ H and $\hbar\nu = 0.047\Phi_0^2/\Lambda$ for $\Phi_x = 0, 0.49$ and $0.5\Phi_0$. Also shown are the probability density functions of the rings wavefunctions displaced by their energy eigenvalues.

where $\varphi_x = \Phi_x/\Phi_0$ is the normalized static bias flux applied to the SQUID ring. We note that the cosine term in the Hamiltonian introduces non-linearities to all orders. We have seen that this property of the SQUID ring introduces highly non-perturbative effects [1, 2] when coupled to other circuit systems. In this paper we show that it also gives rise to Schrödinger cats and squeezing within the ring itself.

From (3) it is apparent that as long as the ratio $\nu : \omega$, and the product $C\omega$ ($= \sqrt{C/\Lambda}$), remain the same the physics of this system is unchanged. We therefore choose values of C and $\hbar\nu$ (or equivalently $I_c = 2e\nu$) that can be attained using currently available micro-fabrication techniques, that are physically sensible and that will lead to SQUID ring systems exhibiting quantum be-

haviour at experimentally accessible temperatures. With these factors in mind we choose the circuit parameters $C = 5 \times 10^{-15}\text{F}$, $\Lambda = 3 \times 10^{-10}\text{H}$ and a sufficiently large value of $\hbar\nu$ ($= 0.047\Phi_0^2/\Lambda$; $I_c = 2\mu\text{A}$) to generate clear wells in the ring potential. Thus, for a thin film Josephson tunnel junction weak link with a 1nm oxide insulator thickness (dielectric constant ≈ 10) a capacitance of $5 \times 10^{-15}\text{F}$ yields junction dimensions $\approx 0.25\mu\text{m}$ square, readily achieved using micro-fabrication. Again, with these dimensions the supercurrent density in the junction is around 4kAcm^{-2} which is perfectly reasonable. Furthermore, with $C = 5 \times 10^{-15}\text{F}$, $\Lambda = 3 \times 10^{-10}\text{H}$, $\omega/2\pi = 130\text{GHz}$, well below the frequency corresponding to the superconducting energy gap in niobium ($\approx 1\text{THz}$), a metal often used in weak link device fabrication. Given these chosen parameter values, and assuming, as our example, SQUID circuits based on niobium, these correspond to $\nu/\omega = 7.9$ and $C\omega = 4.1 \times 10^{-3}$, values which, unless otherwise stated, we now keep to throughout this paper.

Adopting these values of Λ , C and $\hbar\nu$ we show in figure 2 the SQUID ring potential $U(\Phi, \Phi_x) = (\Phi - \Phi_x)^2/2\Lambda - \hbar\nu \cos(2\pi\Phi/\Phi_0)$ - see (1) - computed for three different values of Φ_x ($= 0\Phi_0$ (top), $0.49\Phi_0$ (middle) and $0.5\Phi_0$ (bottom)). We also show in this figure the probability densities of the wavefunctions of the ring as a function of Φ_x . These probability densities are displaced by their energy eigenvalues, found by solving the time independent Schrödinger equation (TISE) using the Hamiltonian (1). As the bottom of each of the local wells in the ring potential in figure 2 is approximately quadratic, we would expect the solutions deep within these wells to look like those for the simple harmonic oscillator. In addition, we find that, on average, these states are slightly squeezed in terms of the magnetic flux variable Φ . For example, in figure 2 the lowest state in each of the wells for $\Phi_x = 0.49\Phi_0$ has $\left(\Delta\left[\sqrt{C\omega/\hbar}\Phi\right]\right)^2 \approx 0.43$ and $\left(\Delta\left[\sqrt{1/C\hbar\omega}Q\right]\right)^2 \approx 0.58$ (compared to 0.5 in the unsqueezed state), where Φ and Q are normalised to $(\hbar/C\omega)^{1/2}$ and $(\hbar C\omega)^{1/2}$, respectively. To aid in the description of the system we adopt the term locally s-harmonic to describe this behaviour, where the prefix *s* denotes the squeezed nature of these states. The equivalence of the low lying set of energy eigenvalues deep in each (local) well is a sound approximation except where the energy levels of two or more wells align. In such cases, of course, symmetric and antisymmetric superpositions of the eigenfunctions for the isolated wells develop.

In figure 3 we show a set of computed SQUID ring energy eigenvalues of the Hamiltonian operator (3), starting with the ground state, as a function of external flux Φ_x and spanning one flux quantum. For clarity the energy levels are shown as alternating black and grey lines. As can be seen, for the values of Λ , C and $\hbar\nu$ we have adopted in this work there exist many crossing points of the original eigenvalues as Φ_x is changed over a Φ_0

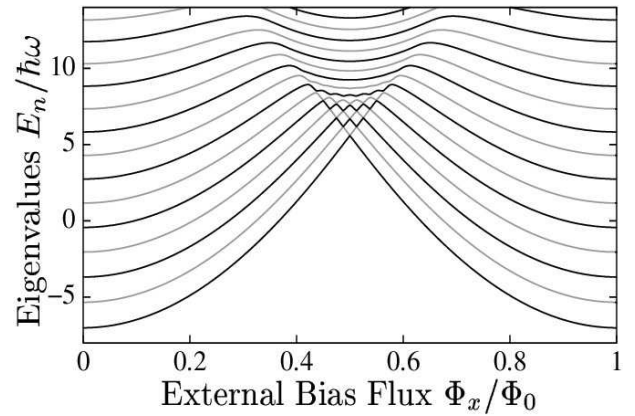


FIG. 3: Computed SQUID ring energy eigenvalues of the Hamiltonian for the SQUID ring of figure 2.

period. At the scale provided in figure 3 these crossing points appear to be degenerate in energy (e.g. in the lowest two eigenvalues at $\Phi_x = 0.5\Phi_0$). Of course, this is not the case, as would be evident if these crossing points were computed to sufficient accuracy. However, for the potential wells shown in figure 2, with the very weak coupling between levels in different wells, the energy splittings at these points may be extremely small indeed.

Results

Schrödinger Cats

Ignoring, for the moment, the special cases where the locally s-harmonic oscillator states are degenerate (zero coupling between wells) we instead consider making a equal superposition of two energy eigenstates. We start by assuming that these two states are locally s-harmonic in different wells and, for simplicity, take these states to correspond to the lowest energy levels in each well. Then, as one would expect, the superposition of these states is a Schrödinger cat state. As this superposition state is no longer an eigenstate of the Hamiltonian for the system, it must evolve with time. This evolution introduces a phase difference between the two stationary (locally s-harmonic) states in the superposition which manifests itself in a time dependent evolution of the interference term in the Wigner function.

In computing Wigner functions for the SQUID ring it is convenient to introduce equivalent dimensionless position (x) and momentum (p) operators in place of Φ and Q . These are defined as

$$x = \sqrt{\frac{C\omega}{\hbar}}\Phi, p = \sqrt{\frac{1}{\hbar C\omega}}Q$$

An example of a Schrödinger cat state in a SQUID ring, as illustrated through its computed Wigner function, is shown in figure 4, both in perspective and in

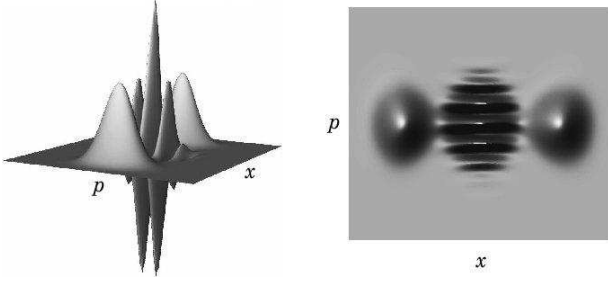


FIG. 4: Wigner function showing, both in perspective and in projection on to the

$x - p$ plane, the Schrödinger cat nature of the superposition state $\frac{1}{\sqrt{2}}(|A\rangle + |B\rangle)$ for the SQUID ring of figure 2.

projection on the $x - p$ plane. Here, we have taken our standard values of Λ , C and $\hbar\nu$ (above) and have selected the state $\frac{1}{\sqrt{2}}(|A\rangle + |B\rangle)$ at the flux bias $\Phi_x = 0.49\Phi_0$ of figure 2(b). In this example we can distinguish in the Wigner function two macroscopically distinct flux states of the SQUID ring in the $x - p$ plane, separated from one another by an oscillatory region. The latter, oscillatory, region arises because of the quantum coherence between the two separate components in the superposition and demonstrates that we are indeed dealing with a true Schrödinger cat state. We note that the Wigner function of figure 4 has been calculated at a fixed time $t = 0$. However, its general form does not vary with time. Nevertheless, there is dynamical evolution of the interference term in the superposition but not in the observable flux states.

Tunable Schrödinger Cats

We now consider the potential with a static bias flux $\Phi_x = 0.5\Phi_0$, as shown in the bottom plot of figure 2. By examining the first two energy eigenstates we find that we have wavefunctions which are a symmetric, $|s\rangle$, and antisymmetric, $|a\rangle$, superposition of the lowest energy, locally s-harmonic, oscillator vacuum states of the two middle wells. These two states are squeezed Schrödinger cats which, due to the large barrier between the wells in the potential, are extremely close in energy. Even so, the interference terms in the Wigner function between the “alive” and “dead” states for each of these Schrödinger cat states are $\pi/2$ out of phase. However, from the viewpoint of theory we might also consider an equal superposition of these states of the form

$$\frac{1}{\sqrt{2}}(|s\rangle + \exp(i\theta)|a\rangle) \quad (4)$$

where θ is the (adjustable) phase. The effect of changing θ can be dramatic, as illustrated in figure 5, where the Wigner function in the $x - p$ plane is shown for selected values of this parameter. As is apparent, when the

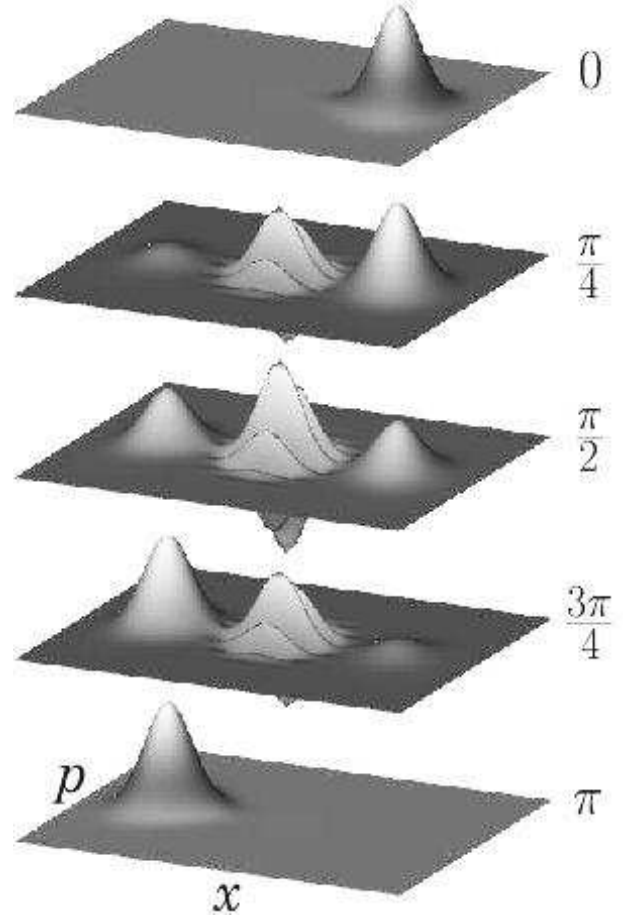


FIG. 5: Wigner function of a superposition of the lowest two (symmetric and anti-symmetric) energy eigenstates as a function of phase - see equation (4) and related text.

wavefunction for the ring is strongly (but not completely) localised in two or more regions in the ring potential it is the quantum interaction between these regions that is responsible for the creation of Schrödinger Cat states.

We note that given the very slightly different energies between the symmetric and antisymmetric superposition states, due to the height of the barrier between the two wells, the superposition (4) will oscillate slowly back and forth between these wells. Using these energies we calculate this period to be 100ns. This is much longer than the time constant corresponding to the ΛC frequency of the SQUID ring in our example (i.e. for $C = 5 \times 10^{-15}\text{F}$, $\Lambda = 3 \times 10^{-10}\text{H}$ this is 7.6ps) but well within the decoherence times of modern SQUID ring circuits [4, 24, 25].

In the above discussion we have considered the development of Schrödinger cat states in a SQUID ring based on a choice of ring parameters which can be realised by fabrication and which are physically reasonable. However, this choice does not connect directly with published experimental data. We will therefore deviate briefly from our standard parameter values and consider an explicit example of superpositions of SQUID ring states as re-

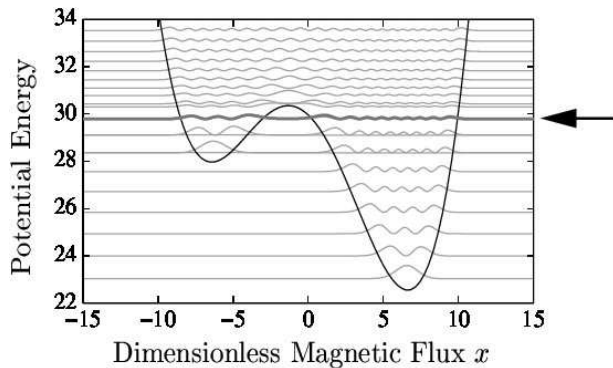


FIG. 6: Potential energy of a SQUID ring with parameter values $C = 1.03 \times 10^{-13} \text{F}$, $\Lambda = 2.38 \times 10^{-10} \text{H}$, $I_c = 2.02 \times 10^{-6} \text{A}$ and $\Phi_x = 0.514466\Phi_0$ (after Friedmann et al [14]). Also shown are the probability density functions of the rings wavefunctions displaced by their energy eigenvalues. The arrow indicates the states used to calculate the superposition state.

ported recently in the literature by Friedman et al [14]. In this paper the authors considered a “*Quantum Superposition of Distinct Macroscopic States*”, namely a Schrödinger cat state, and presented experimental evidence indicating that a SQUID ring could be placed into a superposition of two magnetic flux states. We now demonstrate by computation that this superposition may indeed form a true Schrödinger cat state. The experimental system used a SQUID ring with the circuit parameters $C = 1.03 \times 10^{-13} \text{F}$, $\Lambda = 2.38 \times 10^{-10} \text{H}$ and $I_c = 2.02 \times 10^{-6} \text{A}$. To obtain a superposition state as demonstrated in this paper we used the external bias flux quoted by the authors, i.e. $\Phi_x = 0.514466\Phi_0$. The potential energy of a SQUID ring with these parameters is shown in figure 6 together with the probability densities for the ring wavefunctions. These are displaced, as before, by their energy eigenvalues. In this figure we have marked with an arrow the states in the left hand and right hand wells from which we will form our superpositions. These are the states that were utilised in the Friedman et al experiment.

These eigenfunctions are similar to those of figure 5 in that they form a symmetric, $|s\rangle$, and antisymmetric, $|a\rangle$, superposition of the of the locally s-harmonic states of the separate wells, albeit with higher and different ordinal numbers. The quantum state of the SQUID ring, as reported by Friedman et al. [14] will thus be a superposition of these two eigenstates. For our purposes it is therefore sufficient to look (again) at superpositions of the form

$$\frac{1}{\sqrt{2}} (|s\rangle + \exp(i\theta) |a\rangle). \quad (5)$$

In figure 7 we show the Wigner functions for three different superpositions of these eigenstates, again both in perspective and projection on to the $x - p$ plane. We notice that compared with the Wigner functions of fig-

ure 5 both the states of the Schrödinger cat corresponding to the left and right hand wells in figure 7, and the region of interference between them, display more complex patterns. Given the choice of more highly excited states in the Friedmann et al experiment this is to be expected. Nevertheless, figure 7 demonstrates that the Wigner function (and, of course, the associated Weyl function) can expose sophisticated quantum coherent behaviour in SQUID rings.

Dissipation

In considering the effect of dissipation on the calculations presented in this paper we have chosen to use a standard approach, and one familiar in quantum optics. This is to done by coupling the SQUID ring to a decohering monochromatic thermal bath. The master equation for the evolution of the density operator of the system then takes the form [26],

$$\begin{aligned} \frac{\partial \rho}{\partial t} = & -\frac{i}{\hbar} [\mathcal{H}, \rho] + \frac{\gamma}{2\hbar} (M+1) (2a\rho a^\dagger - a^\dagger a \rho - \rho a^\dagger a) \\ & + \frac{\gamma}{2\hbar} M (2a^\dagger \rho a - a a^\dagger \rho - \rho a a^\dagger). \end{aligned} \quad (6)$$

where M is related to the temperature T and the frequency ω_b of each decohering bath via $M_i = (\exp(\hbar\omega_b/k_B T) - 1)^{-1}$ and γ_i is the coupling (damping rate) between each of the components to its respective thermal bath. For the following examples that we will now calculate we set $T = 1 \text{K}$ with $\omega_b = \omega$.

To illustrate the effect that dissipation has upon a Schrödinger cat state in a SQUID ring, we now solve the master equation (6) for the system evolution, where the ring is taken to be in its ground state at $\Phi_x = 0.5\Phi_0$. For this computation we return to our initial circuit values of $C = 5 \times 10^{-15} \text{F}$, $\Lambda = 3 \times 10^{-10} \text{H}$ and $\hbar\nu = (0.047\Phi_0^2/\Lambda)$. Here we have chosen to use a decoherence rate of 0.01ω . In figure 8 we have plotted the Wigner and Weyl function for the ring at particular times. As the system evolves we notice that the Wigner and Weyl functions display very clearly the disappearance of the quantum coherence between the two states of the cat. We also note that after sufficient time has elapsed the Wigner function still displays two distinct flux probabilities. However, the SQUID ring is longer in a pure state and this represents a classical coin toss probability and not a quantum one. This is also clearly reflected in the disappearance of the symmetrically positioned correlation peaks in the Weyl function at these later times.

Squeezed states of a SQUID ring

Just as in quantum optics, where coherent light can be squeezed in the number-phase plane through its interaction with a non-linear optical medium, so we shall now

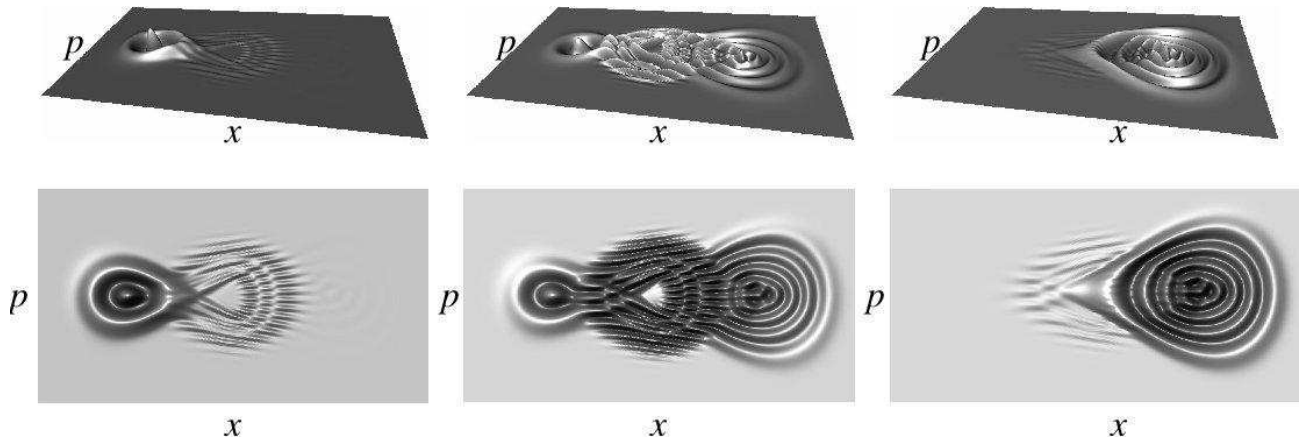


FIG. 7: Wigner function for the three distinct phases $0, \pi/2$ and π (cf. figure 5 and after Friedmann et al [14]), shown from left to right, both in perspective and in projection on to the $x-p$ plane, of the superposition of the (symmetric and anti-symmetric) energy eigenstates as indicated in figure 6.

demonstrate that a SQUID ring, with the cosine Hamiltonian (1), can be used to squeeze an initial coherent state. This starting condition in a SQUID ring can be achieved by changing the weak link structure in the ring. As is well known, the combined Josephson critical current in a parallel, two weak link, loop, connected by superconducting wires (a DC SQUID [27]), can be varied by adjusting the magnetic flux threading the loop. Such a structure can serve as the adjustable weak link within a larger diameter SQUID ring. This has been already been discussed in several earlier papers, including that of Friedman et al [14]. The arrangement is depicted in figure 9. Provided the control magnetic flux (Φ_{x_2}) threading the minor loop in figure 9 is large enough, and the weak links in the loop can be fabricated (in principle) to possess identical critical currents, then the net supercurrent carried through the loop can be made vanishingly small. In this situation the Josephson coupling energy in (1) reduces essentially to zero leaving just the parabolic background term (i.e. as for a simple harmonic oscillator). We take this as the initial prepared condition of the major SQUID ring (with a main control flux Φ_{x_1}) for which we can choose a coherent state $|A = i\sqrt{1}\rangle$. We follow this initial set up by a very rapid reduction in the Φ_{x_2} to yield the desired (and finite) Josephson coupling energy in the principal SQUID ring corresponding to the ring potential considered throughout this paper. Clearly, in an experimental situation this reduction must take place on a time scale short compared with the decoherence time of the SQUID ring coupled to its environment. With this proviso the system is prepared in the required coherent state and then allowed to evolve over time using the master equation (6).

Here, as before, we take the SQUID ring circuit parameters to be $C = 5 \times 10^{-15}\text{F}$ and $\Lambda = 3 \times 10^{-10}\text{H}$. However, in order to improve the effects of squeezing by the ring we have increased $\hbar\nu$ to $0.24\Phi_0^2/\Lambda$, yielding a super-

conducting critical current density of around 20kAcm^{-2} . From our given initial condition, and by computing the uncertainties in flux, we see that the SQUID ring can squeeze the magnetic flux within the ring. We choose not to show the results for the charge as they do not provide any additional information relevant to this discussion. In figure 10 we show the uncertainty in flux for a selection of decoherence rates. Here, the horizontal line denotes that squeezing happens for $(\Delta x)^2$ less than $1/2$. We can clearly see that, on average, the ring has effectively squeezed this state. We also see that for a judicious choice of decoherence rate and interval of time, dissipation can assist in the squeezing process. We note that in the $\gamma = 0.1$ case it can be seen that the SQUID ring decoheres to its (squeezed) vacuum state over a relatively short period. Thus, it appears that these potential wells may be used with facility to generate squeezing of the the magnetic flux variable of the ring. It is therefore reasonable to assume that adiabatic changes of this potential would, unless matching conditions exist between local s-harmonic energy levels of adjacent wells, allow some adjustment of the expectation value of the flux in the ring.

Conclusions

In this paper we have explored two applications of SQUID rings, with strong analogies to the field of quantum optics, which may prove to be of great utility given the current interest in quantum circuit technologies. In the first we describe the manner in which we can create Schrödinger cat states in SQUID rings and the way these may be manipulated through an external control flux. In the second we provide a dynamical mechanism for inducing squeezing of the magnetic flux variable in a SQUID ring starting from an almost harmonic oscillator state.

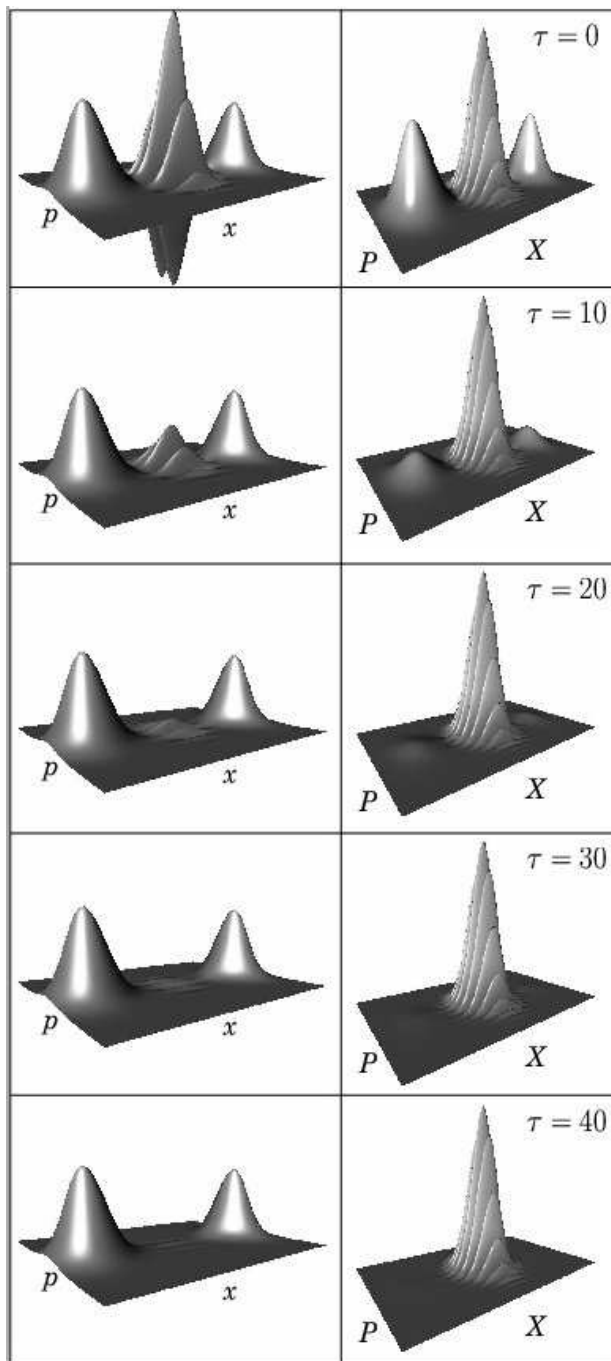


FIG. 8: Wigner (left) and Weyl (right) functions for the ground state of the SQUID ring of 3 evolving in the presence of dissipation ($T = 1\text{K}$ and $\gamma = 0.01\omega$). The effect of dissipation is to remove the quantum correlations in the Schrödinger cat state over the time shown.

These take advantage of the highly non-perturbative quantum nature of SQUID rings arising from the cosine coupling energy term in the ring Hamiltonian. As we emphasise, both are of great interest in the light of current research in the fields of quantum computing and

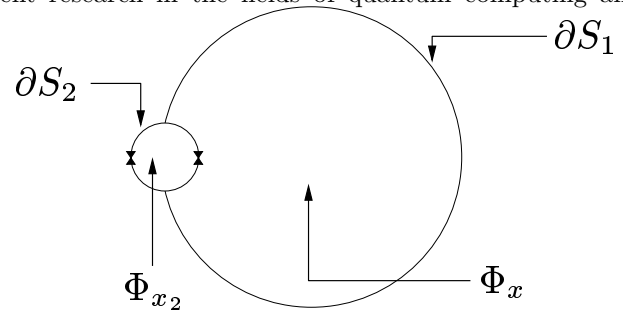


FIG. 9: Schematic of a SQUID ring with a (flux) controllable Josephson tunnelling energy. Here the area enclosed by the outer loop ∂S_1 is much greater than that enclosed by the inner loop ∂S_2 .

quantum information processing [10, 11, 12, 13]. Moreover, the results presented in this paper emphasise that the SQUID ring can act as a versatile quantum device and, as we have shown previously, can be used to create correlations across extended, multi-component, quantum circuit systems [1, 2, 28, 29, 30, 31]. These correlations can, for example, be made manifest as quantum entanglements and quantum frequency up/down conversion [1, 2], with each controlled by the external bias flux applied to the SQUID ring. In this sense these phenomena, including Schrödinger cat states and squeezing, highlight the role of the SQUID ring as the essential machinery for a range of applications in superconducting quantum circuit technologies. This further enhances our understanding of these non-perturbative quantum objects and their possible usefulness in these incipient technologies.

Acknowledgements

We would like to thank the EPSRC for its generous funding of this work and for sponsoring the U.K. Quantum Circuits Network. We would also like to express our thanks both to Professors C.H. van de Wal and A. Sobolev for interesting discussions and to the Sussex High Performance Computing Initiative for the use of their NAG-IRIS explorer graphics software.

[1] M. J. Everitt, P. Stiffell, T. D. Clark, A. Vourdas, J. F. Ralph, H. Prance, and R. J. Prance, Phys. Rev. B **63**14, art. no. (2001).

[2] M. J. Everitt, T. D. Clark, P. Stiffell, H. Prance, R. J. Prance, A. Vourdas, and J. F. Ralph, Phys. Rev. B **64**18, art. no. (2001).

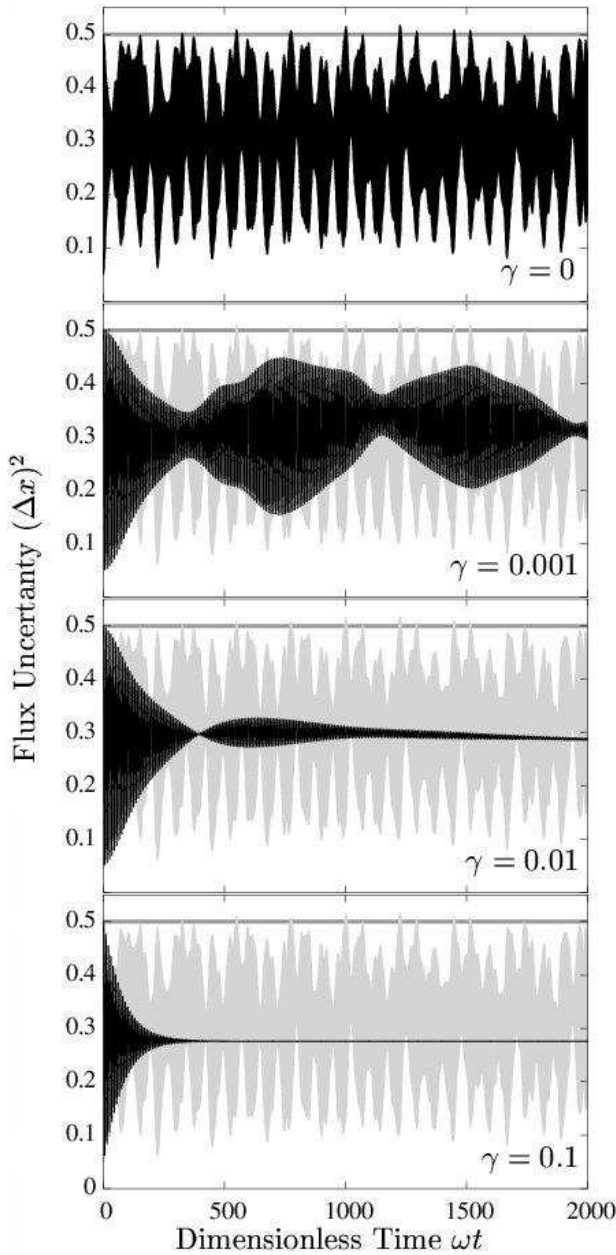


FIG. 10: Uncertainty in dimensionless flux, for a SQUID ring with parameter values $C = 5 \times 10^{-15} \text{F}$, $\Lambda = 3 \times 10^{-10} \text{H}$ and $\hbar\nu = 0.24\Phi_0^2/\Lambda$, computed for a selection of decoherence rates at $T = 1\text{K}$. Here the horizontal line denotes that squeezing occurs for $(\Delta x)^2$ less than $1/2$. The grey background oscillation for the $\gamma = 0.001, 0.01$ and 0.1 examples is the $\gamma = 0$ pattern repeated for comparison.

[3] I. Chiorescu, Y. Nakamura, C. Harmans, and J. Mooij, *Science* **299**(5614), 1869 (2003).
 [4] J. Martinis, S. Nam, and J. Aumentado, *Phys. Rev. Lett.* **89**(11), 117901 (2002).
 [5] R. Rouse, S. Y. Han, and J. E. Lukens, *Phys. Rev. Lett.*

75, 1614 (1995).
 [6] P. Silvestrini, B. B. Ruggiero, C. Granata, and E. Esposito, *Phys. Lett. A* **267**, 45 (2000).
 [7] Y. Nakamura, C. D. Chen, and J. S. Tsai, *Phys. Rev. Lett.* **79**, 2328 (1997).
 [8] Y. Nakamura, Y. A. Pashkin, and J. S. Tsai, *Nature* **398**, 786 (1999).
 [9] C. H. van der Wal, A. C. J. ter Haar, F. K. Wilhelm, R. N. Schouten, C. J. P. M. Harmans, T. P. Orlando, S. Lloyd, and J. E. Mooij, *Science* **290**, 773 (2000).
 [10] H. Lo, S. Popescu, and T. Spiller, eds., *Introduction to Quantum Computation and Information* (World Scientific, New Jersey, 1998).
 [11] T. P. Orlando, J. E. Mooij, L. Tian, C. H. van der Wal, L. S. Levitov, S. Lloyd, and J. J. Mazo, *Phys. Rev. B-Condens Matter* **60**, 15398 (1999).
 [12] Y. Makhlin, G. Schon, and A. Shnirman, *Nature* **398**, 305 (1999).
 [13] D. V. Averin, Y. V. Nazarov, and A. A. Odintsov, *Physica B* **165**, 945 (1990).
 [14] J. R. Friedman, V. Patel, W. Chen, S. K. Tolpygo, and J. E. Lukens, *Nature* **406**, 43 (2000).
 [15] T. Spiller, T. Clark, R. Prance, and A. Widom, *Progress in Low Temperature Physics*, vol. XIII (Elsevier Science Publishers, 1992).
 [16] E. Wigner, *Physical Review* **40**, 749 (1932).
 [17] N. L. Balazs and B. K. Jennings, *Physics Reports* **104**, 347 (1984).
 [18] C. Chountasis and A. Vourdas, *Phys. Rev. A* **58**(2), 848 (1998).
 [19] W. Schleich, *Quantum Optics in Phase Space* (WILEY-VCH, Berlin, Germany., 2001).
 [20] Y. Srivastava and A. Widom, *Phys. Reports-Review Section Physics Letters* **148**, 1 (1987).
 [21] A. J. Leggett, S. Chakravarty, A. T. Dorsey, M. P. A. Fisher, A. Garg, and W. Zwerger, *Rev. Mod. Phys.* **59**, 1 (1987).
 [22] T. D. Clark, J. Diggins, J. F. Ralph, M. Everitt, R. J. Prance, H. Prance, R. Whiteman, A. Widom, and Y. N. Srivastava, *Ann. Phys.* **268**, 1 (1998).
 [23] J. Diggins, R. Whiteman, T. D. Clark, R. J. Prance, H. Prance, J. F. Ralph, A. Widom, and Y. N. Srivastava, *Physica B* **233**, 8 (1997).
 [24] S. Zhou, S. Chu, and S. Han, *Phys. Rev. B.* **66**, 054527 (2002).
 [25] S. Han, Y. Yu, S. Chu, and Z. Wang, *Science* **293**, 1457 (2001).
 [26] U. Weiss, *Quantum Dissipative Systems* (World Scientific, 1999).
 [27] K. K. Likharev, *Dynamics of Josephson Junctions and Circuits* (Gordon And Breach, 1986).
 [28] R. Migliore and A. Messina, *Phys. Rev. B.* **67**(13), 134505 (2003).
 [29] R. Migliore and A. Messina, *Int. J. Mod. Phys. B.* **17**(4-6), 709 (2003).
 [30] E. Almaas and D. Stroud, *Phys. Rev. B* **65**(13), 134502 (2002).
 [31] W. Al-Saidi and D. Stroud, *Phys. Rev. B* **65**(1), 014512 (2002).